Actin Filament Barbed End Elongation with Nonmuscle MgATP−Actin and MgADP−Actin in the Presence of Profilin[†]

Henry J. Kinosian,*[,‡,§] Lynn A. Selden,[§] Lewis C. Gershman,[§,||] and James E. Estes[‡,§]

Center for Cell Biology and Cancer Research and Department of Medicine, Albany Medical College, Albany, New York 12208, and Research Service and Medical Service, Stratton VA Medical Center, Albany, New York 12208

Received December 21, 2001; Revised Manuscript Received March 20, 2002

ABSTRACT: We have quantitated the in vitro interactions of profilin and the profilin−actin complex (PA) with the actin filament barbed end using profilin and nonmuscle β,γ-actin prepared from bovine spleen. Actin filament barbed end elongation was initiated from spectrin seeds in the presence of varying profilin concentrations and followed by light scattering. We find that profilin inhibits actin polymerization and that this effect is much more pronounced for β,γ-actin than for α-skeletal muscle actin. Profilin binds to β,γ-actin filament barbed ends with an equilibrium constant of 20 μM, decreases the filament elongation rate by blocking addition of actin monomers, and increases the dissociation rate of actin monomers from the filament end. PA containing bound MgADP supports elongation of the actin filament barbed end, indicating that ATP hydrolysis is not necessary for PA elongation of filaments. Initial analysis of the energetics for these reactions suggested an apparent greater negative free energy change for actin filament elongation from PA than elongation from monomeric actin. However, we calculate that the free energy changes for the two elongation pathways are equal if the profilin-induced weakening of nucleotide binding to actin is taken into consideration.

Profilin is a small (∼15 kDa) actin-binding protein, ubiquitous in eukaryotes, that has been implicated in the control of actin polymerization and cytoskeletal reorganization in vivo (*1*−*3*). Profilin binds to the barbed end of the actin monomer (*4*) between subdomains 1 and 3 and increases the rate constant for nucleotide exchange on actin (*5*). Profilin desequesters actin monomers bound to thymosin β4, allowing actin filament barbed end elongation (*6*), and profilin enhances actin filament turnover in the presence of ADF/cofilin (*7*). Profilin recruits monomeric MgATP−actin to areas of actin filament growth via interactions with N-WASP (*1*, *2*) and VASP (*8*−*11*). When the actin filament barbed ends are capped by other actin-binding proteins, profilin acts as an actin-sequestering protein. When actin filament barbed ends become uncapped, the profilin-catalyzed formation of MgATP−actin from MgADP−actin delivers a homogeneous supply of MgATP−actin to the growing filament barbed end (*12*−*14*).

In the presence of profilin, actin filament elongation can take place through two pathways, as depicted in Scheme 1 (*6*, *15*). One pathway is the simple addition of monomeric actin subunits onto actin filament ends (AF pathway). The other pathway is via addition of the profilin−actin complex (PA)[1] onto the actin filament barbed ends followed by the dissociation of profilin from the filament end (PAF pathway); the strength of the profilin−actin bond is greatly decreased after PA associates with an actin filament end. Four

Scheme 1: Pathways for Actin Elongation in the Presence of Profilin[a]

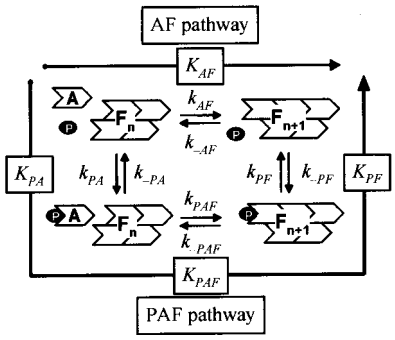

[a] Actin filaments (F_n) elongate by the simple addition of actin monomers (A) onto the actin filament barbed end through the AF pathway. In the PAF pathway, the profilin−actin complex (PA) elongates actin filaments through three consecutive reactions: (1) profilin (P) binds monomeric actin to form PA; (2) PA associates with the actin filament barbed end; and (3) profilin dissociates from the actin filament barbed end. If the model is correct, the free energy change for each pathway must be equal. Values determined for the rate and equilibrium constants are listed in Tables 1 and 2.

[†] This work was supported by Department of Veterans Affairs Grants 1912-0001 (J.E.E.) and 0398-0002 (L.C.G.).

* To whom correspondence should be addressed at Research Service, Mail Code 151, Stratton VA Medical Center, 113 Holland Ave., Albany, NY 12208. Phone: (518) 626-5644; fax: (518) 626-5628; e-mail: henry.kinosian@med.va.gov.

[‡] Center for Cell Biology and Cancer Research, Albany Medical College.

[§] Research Service, Stratton VA Medical Center.

[||] Department of Medicine, Albany Medical College, and Medical Service, Stratton VA Medical Center.

[1] Abbreviations: PA, profilin−actin complex; TRITC-phalloidin, tetramethylrhodamine isothiocyanate phalloidin; PIP_2, phosphatidylinositol 4,5-bisphosphate.

10.1021/bi016083t CCC: $22.00
Published on Web 05/02/2002

equilibrium constants are needed to describe the two linked actin polymerization pathways: (1) the actin critical concentration; (2) the affinity of profilin for monomeric actin; (3) the affinity of profilin for the actin filament barbed end; and (4) the affinity of PA for the actin filament barbed end. The first two of these constants are independent of each other and may be measured separately; however, measurements of the latter two constants are more difficult to separate experimentally. Literature values for the affinities of profilin or PA for the actin filament barbed end vary by orders of magnitude (*6, 15*−*17*).

Whether these two pathways are energetically equal is a point of contention in the literature at present. It has been proposed that profilin promotes actin polymerization because of a greater negative free energy change ($-\Delta G$) calculated for the actin filament elongation by PA (*6*). The greater $-\Delta G$ in that model was thought to be due to the coupling of actin ATP hydrolysis and PA elongation, and this coupling was required for filament growth by PA (*6, 18*). Other investigators have reported that the two pathways are energetically consistent (*16, 17*), implying that no additional energy input from ATP hydrolysis would be needed to explain the effects of profilin on actin filament elongation.

Previous investigations of PA elongation based on Scheme 1 used either *Acanthameoba* or skeletal muscle α-actin. Work using mammalian profilin and nonmuscle β,γ-actin (*19*) did not analyze actin elongation using Scheme 1, but did report that profilin slowed the rate of actin polymerization and suggested that profilin−actin dissociated faster from the actin filament barbed end than did actin alone. In higher eukaryotes, the leading edge of moving cells is thought to contain predominantly the nonmuscle β-isoform of actin (*20, 21*); therefore, in the present study, we have investigated the effect of profilin on the elongation of nonmuscle β,γ-actin [containing ∼70% β-actin (*22*)]. Using nonmuscle MgATP−actin, we measured the constants for profilin and PA interaction with the actin filament barbed end by employing experimental protocols designed to optimize the determination of each constant. We find that profilin binds to the β,γ-actin filament barbed end with a 20 μM dissociation constant and prevents filament elongation. The data also indicate that profilin bound to the actin filament barbed end weakens the affinity of the terminal actin subunit for the filament end. Moreover, actin-bound ATP hydrolysis is not necessary for PA elongation. Using our independently derived constants, we find that global kinetic simulations of actin elongation over a range of profilin concentrations describe the experimentally observed elongation data well. Analysis of the energetics for Scheme 1 reveals that the free energy changes for the two elongation pathways are equal if the profilin-induced weakening of nucleotide binding to actin (*5*) is taken into consideration.

MATERIALS AND METHODS

Materials. Hexokinase, luciferase−luciferin reagent, TRITC-phalloidin, DNase I, and ATP were from Sigma. Pyrene iodoacetamide was from Molecular Probes.

Protein Preparation. Nonmuscle actin and profilin were prepared from bovine spleen (*5*). Skeletal muscle α-actin was prepared from rabbit skeletal muscle (*23*). Pyrene-labeled nonmuscle actin was prepared by the method of Kouyama and Mihashi (*24*). ADP−actin was prepared using hexokinase and glucose (*25*); the absence of ATP was verified using a luciferase−luciferin assay. Spectrin seeds were prepared from human erythrocytes (*26, 27*).

Actin Polymerization Measurements. Actin polymerization was measured using light scattering at 400 nm or pyrene fluorescence with excitation and emission wavelengths of 365 and 386 nm, respectively (*24*). Prior to polymerization experiments, CaATP−actin was converted to MgATP−actin by a brief incubation with 100−500 μM EGTA (enough to be in excess of Ca^{2+} present) and 50 μM $MgCl_2$. Monomeric actin was diluted to the desired concentrations into buffer containing 10 mM MOPS, pH 7.0, 0.2 mM ATP, or 1 mM ADP (G-buffer), and elongation of actin barbed filament ends was initiated by the addition of 100 mM KCl and 2 mM $MgCl_2$ (F-buffer), and spectrin seeds (about 0.2−2 nM final concentration). For some experiments, F-actin capped by spectrin seeds was added to F-buffer containing varying amounts of monomeric actin. For depolymerization experiments, F-actin capped by spectrin seeds was added to F-buffer containing 1 μM DNase I.

The steady-state actin polymer concentration was assayed using TRITC-phalloidin based on the report of De La Cruz and Pollard (*28*) that showed the observed rate constant for 10 nM TRITC-phalloidin binding to F-actin is proportional to the F-actin concentration. A stock solution was made of 100 μM TRITC-phalloidin in ethanol and was stored at −20 °C. As needed, the TRITC-phalloidin was diluted to 10 μM in 10 mM MOPS, pH 7.3, and a small aliquot of this solution (25 nM final concentration) was added to an F-actin sample and the time course of fluorescence intensity was recorded using excitation and emission wavelengths of 540 and 580 nm, respectively. The observed exponential rate constant for TRITC-phalloidin binding to F-actin was determined from a fit with a single-exponential function to the time course data and is proportional to the concentration of F-actin. Known concentrations of F-actin polymer were used to calibrate the TRITC-phalloidin rate constants. The second-order rate constant for TRITC-phalloidin binding to F-actin was found to be in the range of 0.01−0.02 μM^{-1} s^{-1} depending on buffer conditions and actin isoforms.

Data Analysis in the Absence of Profilin. The light scattering intensity or pyrene fluorescence time course data for actin polymerization were fit with a single-exponential function:

$$I(t) = I_0 + \Delta I(1 - e^{-k_{obs}t}) \quad (1)$$

where I_0 is the initial intensity, ΔI is the change in intensity upon polymerization, and k_{obs} is the observed exponential rate constant. In the absence of profilin, $k_{obs} = [F]k_{AF}$, where [F] is the concentration of actin filament barbed ends and k_{AF} is the actin association rate constant. Control experiments (data not shown) indicate that the k_{AF} value for β,γ-actin was very similar to that for skeletal muscle α-actin which has been previously determined using electron microscopy (*29*), so an absolute value of 10^7 M^{-1} s^{-1} was used for the β,γ-actin k_{AF} value. The total concentration of actin filament barbed ends present after addition of spectrin seeds was assayed using fits to MgATP−actin elongation time course data with eq 1 where $[F_{tot}] = k_{obs}/k_{AF}$ and $k_{AF} = 10^7$ M^{-1} s^{-1} (*29*). Control samples of MgATP−actin were also used to

calibrate the specific intensity change per micromolar of actin polymer, ΔI_{sp}. Initial elongation rates, J, of experimental samples were determined from

$$J = \frac{\Delta I}{\Delta I_{sp}} \cdot \frac{k_{obs}}{[F_{tot}]} \quad (2)$$

Scheme 1 describes the previously established reaction scheme for actin polymerization in the presence of profilin (*6, 17*). The elongation rate for actin, A, shown in Scheme 1 (AF pathway) is described by

$$J = k_{AF}[A] - k_{-AF} \quad (3)$$

Data Analysis in the Presence of Profilin. Analysis of actin filament elongation in the presence of profilin requires the calculation of profilin binding to two ligands, monomeric actin and the actin filament barbed end, resulting in the formation of the profilin−actin complex, PA, and the profilin-capped actin filament barbed end, PF. Because for some experiments the concentrations of profilin and actin are in the same range, the total and free concentrations of profilin cannot be considered equal, a quadratic binding equation is used to calculate [PA]:

$$[PA] = \frac{[P_{tot}] + [A_{tot}] + K_{PA} - \sqrt{([P_{tot}] + [A_{tot}] + K_{PA})^2 - 4[P_{tot}][A_{tot}]}}{2} \quad (4)$$

where $[A_{tot}]$ and $[P_{tot}]$ are the total monomeric actin and profilin concentrations, respectively, and for MgATP−actin, $K_{PA} = 0.1\ \mu$M (*5*) is the equilibrium dissociation constant for profilin binding to monomeric actin. However, because the concentration of profilin is in large molar excess over the concentration of actin filament barbed ends, the total profilin concentration can be considered to equal the free profilin concentration, and a hyperbolic function is used to calculate [PF]:

$$[PF] = [F_{tot}]\frac{[P]}{[P] + K_{PF}} \quad (5)$$

where K_{PF} is the equilibrium dissociation constant for profilin binding to the actin filament barbed end. Since the equilibrium constants for profilin binding to monomeric actin and to actin filament barbed ends are different by a factor of 200, $K_{PF} = 20\ \mu$M (Figure 3) and $K_{PA} = 0.1\ \mu$M, the binding of profilin to monomer or to filaments can be considered independently.

In the presence of profilin, the elongation time courses for MgATP−actin are well described by a single-exponential function (eq 1); however, to analyze k_{obs} from an exponential fit to the elongation time course, we must establish that changes in the free profilin concentration during elongation do not significantly alter the elongation time course. Since the addition of PA to the growing actin filament releases profilin, this free profilin may rebind either to monomeric actin or to the actin filament barbed end, thereby altering the concentration of free actin or free barbed ends. The formation of PA during the elongation time course will not alter k_{obs} if the association rate constants for actin and for PA are approximately equal. This is shown to be the case in the experiments depicted in Figure 3, in which increasing the profilin concentration from zero to equimolar with the 1 μM MgATP−actin results in a change of only about 10% in k_{obs}. Profilin released from PA during actin filament elongation may also rebind to the actin filament barbed end, but if the increase in the free profilin concentration is much smaller than the equilibrium dissociation constant for profilin binding to the actin filament barbed end, K_{PF}, then the concentration of free barbed ends will not be significantly changed. This condition is met for the elongation of 1 μM MgATP−actin determined from the experiments shown in Figures 2 and 3 that indicate $K_{PF} = 20\ \mu$M. For example, in Figure 3, elongation of 1 μM MgATP−actin in the presence of 1 μM profilin results in the liberation of about 0.73 μM profilin during the elongation time course, which would result in binding to only 3.5% of the actin filament barbed ends. Thus, in the presence of profilin, the observed elongation rate constant, k_{obs}, can be described by

$$k_{obs} = [F]\left(\frac{k_{AF}[A] + k_{PAF}[PA]}{[A_{tot}]}\right) \quad (6)$$

Given that $k_{AF} \approx k_{PAF}$ (from Figure 3) and $[A] + [PA] = [A_{tot}]$, eq 6 reduces to $k_{obs} = [F]k_{AF}$, and, therefore, k_{obs} is proportional to the concentration of free barbed ends, [F]. When k_{obs} is normalized to a maximal value of 1 at 0 profilin concentration (Figure 3B), the *normalized* k_{obs} can be described by

$$\textit{normalized}\ k_{obs} = 1 - \frac{[P]}{[P] + K_{PF}} \quad (7)$$

For initial elongation rate determinations, the concentrations of the reactants are well-defined. In the presence of profilin, the initial elongation rate is a combination of elongation from A and PA and is described by

$$J = \frac{[F](k_{AF}[A] - k_{-AF} + k_{PAF}[PA]) - k_{-PAF}[PF]}{[F_{tot}]} \quad (8)$$

where k_{AF} and k_{-AF} are rate constants for actin elongation and dissociation, respectively; k_{PAF} and k_{-PAF} are rate constants for profilin−actin elongation and dissociation, respectively; $[F_{tot}]$, [F], and [PF] are the total, free, and profilin-bound actin filament barbed end concentrations, respectively. When no monomeric actin is present to associate to an actin filament, as is the case for the depolymerization of F-actin in the presence of DNase I (Figure 4) (*30*), eq 6 reduces to

$$J = \frac{-k_{-AF}[F] - k_{-PAF}[PF]}{[F_{tot}]} = -k_{-AF}\left(1 - \frac{[P]}{[P] + K_{PF}}\right) - k_{-PAF}\left(\frac{[P]}{[P] + K_{PF}}\right) \quad (9)$$

Data Analysis: A Global Kinetic Model. An alternative analysis of the actin filament elongation data was also used. A series of differential equations based on Scheme 1 were used to describe the nucleated actin polymerization time courses in the presence of profilin. This global kinetic analysis was used to corroborate the rate constants deter-

mined for elongation of MgATP−actin in the presence of varying concentrations of profilin, and, additionally, to analyze data for elongation of MgADP−actin in the presence of profilin. The simplifying assumption that the elongation rate constants for MgADP−actin and for profilin−MgADP−actin are approximately equal could not be made. Nor could the MgADP−actin be elongated in the presence of high enough concentrations of profilin to consider the free profilin concentration constant during the time course of elongation.

The initial preequilibrium concentrations [A], [PA], and [PF] were calculated using eqs 4 and 5, and the time courses for [A], [PA], and [PF] were calculated using eqs 10, 11, and 12, respectively. The time courses for [F-actin], [F], and [P] were determined from eqs 13, 14, and 15, respectively.

$$\frac{d[A]}{dt} = -k_{AF}[A][F] + k_{-AF}[F] - k_{PA}[A][P] + k_{-PA}[PA] \quad (10)$$

$$\frac{d[PA]}{dt} = -k_{PAF}[PA][F] + k_{-PAF}[PF] + k_{PA}[A][P] - k_{-PA}[PA] \quad (11)$$

$$\frac{d[PF]}{dt} = k_{PAF}[PA][F] - k_{-PAF}[PF] + k_{PF}[P][F] - k_{-PF}[PF] \quad (12)$$

$$[F\cdot actin] = [A_{tot}] - [A] - [PA] \quad (13)$$

$$[F] = [F_{tot}] - [PF] \quad (14)$$

$$[P] = [P_{tot}] - [PA] - [PF] \quad (15)$$

RESULTS

Profilin Attenuates Polymerization of Nonmuscle Actin More than Muscle Actin. The effect of profilin on actin polymerization was studied using spectrin seeds to nucleate actin filament barbed end growth. Figure 1A shows time course data for barbed end elongation of skeletal muscle α-actin (triangles) and nonmuscle β,γ-actin (circles) with and without profilin. Figure 1B shows the steady-state concentrations of polymerized skeletal muscle α-actin (triangles) and nonmuscle β,γ-actin (circles) incubated overnight in the presence of varying profilin concentrations, measured by TRITC-phalloidin binding (see Materials and Methods for details). We obtained very similar results when aliquots of the steady-state samples were centrifuged and the supernatants analyzed by densitometry of Coomassie blue stained SDS−PAGE gels; the actin concentration in the supernatants increased with increasing profilin concentration, indicating an inhibition of actin filament formation (data not shown). The lines in Figure 1B are linear regressions to the data and extrapolate to a critical actin concentration of 0.1 μM for both actin isoforms in the absence of profilin. The rate and extent of skeletal muscle α-MgATP−actin polymerization are only slightly affected by the presence of ≤20 μM profilin, similar to previous reports using skeletal muscle α-actin (*16*, *31*). In contrast, both the rate and extent of polymerization of 1 μM β,γ-MgATP−actin are decreased by 20 μM profilin to less than 50% of control values. Experiments from other laboratories using *Acanthamoeba* actin and profilin (*15*, *17*) reveal a qualitatively similar but weaker inhibition of actin filament elongation than we find for mammalian cytoplasmic profilin and actin. It should be noted that since profilin inhibits polymer formation from actin, profilin cannot be considered to promote actin polymerization in the absence of other actin-binding proteins such as thymosin β4.

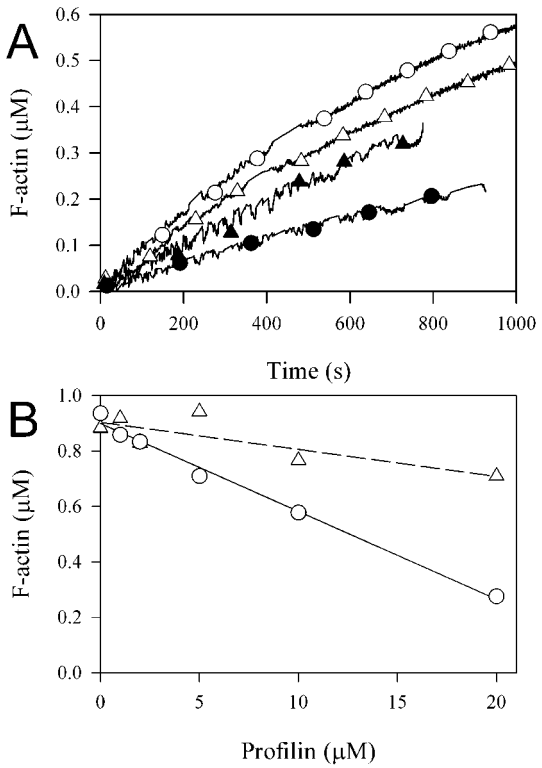

FIGURE 1: Profilin affects polymerization of nonmuscle actin more strongly than elongation of muscle actin. Elongation of 1 μM MgATP−actin was initiated by the addition of spectrin seeds, 100 mM KCl, and 2 mM $MgCl_2$. (A) Time courses for elongation followed by light scattering for nonmuscle β,γ-MgATP−actin (○,●) and skeletal muscle α-MgATP−actin (△,▲) in the absence (○,△) or presence (●,▲) of 20 μM profilin. (B) Steady-state F-actin concentration incubated 18 h in the presence of varying profilin concentrations, measured using TRITC-phalloidin binding (see Materials and Methods for details). Data are for nonmuscle β,γ-MgATP−actin (○) and skeletal muscle α-MgATP−actin (△). The lines are linear regressions to the data which extrapolate to a critical actin concentration of 0.1 μM for both actin isoforms at 0 profilin concentration.

Profilin Decreases the Actin Elongation Rate at Actin Filament Barbed Ends. Figure 2 shows barbed end elongation rate plots for nonmuscle MgATP−actin with and without 20 μM profilin. In the absence of profilin (open circles), elongation rate measurements plotted as a function of actin concentration yield values for the rate constants for elongation, k_{AF}, and depolymerization, k_{-AF}, from the linear slope and intercept with the ordinate, respectively (eq 3). The steady-state concentration of unpolymerized actin, c_{ss}, is indicated by the intercept with the abscissa.

In the presence of profilin, analysis of the J function is more complex and is described by eq 8. Since the 20 μM profilin is in molar excess above the actin concentration, and is much greater than K_{PA} = 0.1 μM, the actin can be considered saturated with profilin. Thus, the contribution to elongation from free actin can be neglected, and from eq 8, the slope of the plot becomes equal to $k_{PAF}[F]/[F_{tot}]$. In the

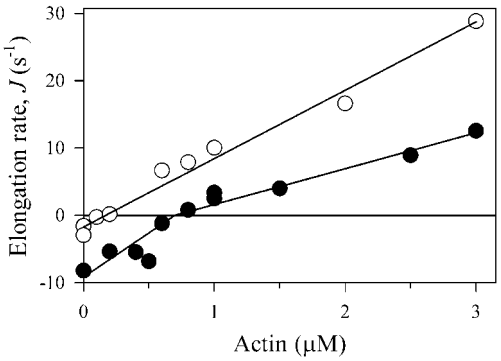

FIGURE 2: Profilin slows the rate of actin filament barbed end elongation. β,γ-MgATP−actin elongation was initiated by the addition of spectrin seeds, 100 mM KCl, and 2 mM $MgCl_2$ in the absence (○) or presence (●) of 20 μM profilin, and varying actin concentrations. In the absence of profilin, linear regression of data at actin concentrations above the critical concentration yields k_{AF} = 10 (±0.8) μM^{-1} s^{-1}, k_{-AF} = 1.7 (±1.3) s^{-1}, and c_{ss} = 0.17 (±0.14) μM. In the presence of 20 μM profilin, linear regression yields a value for the slope $k_{PAF}[F]/[F_{tot}]$ = 5.3 (±0.5) μM^{-1} s^{-1}, a value for the extrapolated intercept with the ordinate 3.7 (±1.0) s^{-1}, and c_{ss} = 0.70 (±0.25) μM. In the presence of 20 μM profilin, linear regression of data below c_{ss} yields an intercept with the ordinate that indicates the observed rate constant for depolymerization of MgADP−actin and the profilin−MgADP−actin complex, equal to 9.2 (±2.3) s^{-1}.

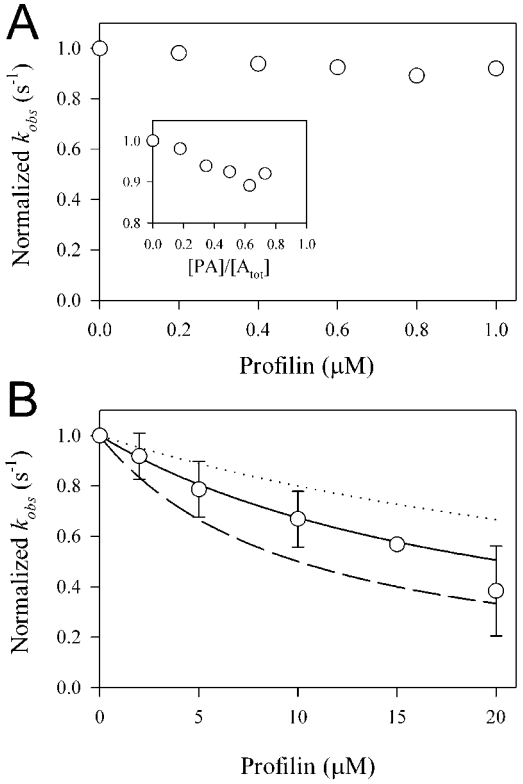

FIGURE 3: Profilin binds to the actin filament barbed end and blocks elongation. Elongation of 1 μM MgATP−actin was initiated by the addition of spectrin seeds, 100 mM KCl, and 2 mM $MgCl_2$ in the presence of varying profilin concentrations, and the observed exponential rate constant, k_{obs}, was derived from curve fits to the time courses. The values for k_{obs} were normalized and plotted versus the total profilin concentration. (A) Profilin concentrations less than or equal to the actin concentration. The inset shows the same normalized k_{obs} values plotted versus the fractional saturation of actin with profilin. (B) Profilin concentrations greater than the actin concentration. Error bars represent the standard deviation of 2−5 measurements. Lines are calculated using eq 9 and varying values for the equilibrium dissociation constant for profilin binding to the actin filament barbed end, K_{PF}: dotted line, 40 μM; solid line, 20 μM; dashed line, 10 μM.

presence of 20 μM profilin (filled circles), the slope of the plot is reduced by approximately 50%; however, the data do not differentiate between a reduced value for the second-order association rate constant, k_{PAF}, or a reduced number of free barbed ends, [F].

The data in Figure 2 also indicate that the addition of profilin increases the c_{ss} from 0.17 to 0.7 μM. This increase in c_{ss} is greater than can be explained by a 50% decrease in k_{PAF} or [F], and suggests that the presence of profilin also increases the dissociation rate constant for PA from the actin filament. The nonlinearity of the rate plot below c_{ss} occurs because actin containing bound MgADP dissociates from the actin filament (*32*); thus, the elongation rate at 0 actin monomer concentration represents the dissociation rate constant for MgADP−actin and profilin−MgADP−actin with a value 9.2 (±2.3) s^{-1}.

Profilin Blocks Elongation at the Actin Filament Barbed End. To differentiate between the two different effects of profilin, barbed end blocking and reducing the PA association rate constant (k_{PAF}), 1 μM β,γ-MgATP−actin was polymerized from spectrin seeds and k_{obs} measured (eq 1). If PA has a slower association rate constant than does actin, then k_{obs} will decrease with increasing profilin concentration following the formation of PA. Figure 3A shows that the addition of profilin to a concentration equimolar with the 1 μM β,γ-MgATP−actin decreases k_{obs} by only about 10%. The inset of Figure 3A depicts the same k_{obs} data plotted as a function of the fractional saturation of actin with profilin, [PA]/[A_{tot}], and shows that at about 75% saturation k_{obs} is about 90% of the control value without profilin. The association rate constant for PA with the actin filament barbed end is similar to that for monomeric actin alone, in agreement with other reports (*6, 15*−*17*).

At profilin concentrations much greater than the 1 μM actin concentration, the monomeric actin can be considered saturated with profilin; thus, any further effect of profilin on k_{obs} must be due to profilin binding to and blocking actin filament barbed ends. Figure 3B shows normalized k_{obs} values for elongation of 1 μM β,γ-MgATP−actin in the presence of varying concentrations of profilin in molar excess of the actin concentration. The lines are calculated using eq 7 with different values for K_{PF}, the equilibrium dissociation constant for profilin binding to the actin filament barbed end: dotted line, K_{PF} = 40 μM; solid line, K_{PF} = 20 μM; dashed line, K_{PF} = 10 μM. The value for K_{PF} = 20 μM is consistent with the observation from Figure 2 that the presence of 20 μM profilin decreases the observed rate of actin filament elongation by about 50%, suggesting that the actin filament barbed ends are half-saturated with profilin which blocks elongation of the filaments.

Using the equilibrium and association rate constants for profilin binding to the actin filament barbed ends, we can estimate the corresponding dissociation rate constant. We have previously published the association rate constant for profilin binding to monomeric β,γ-MgATP−actin, k_{PF} = 15 μM^{-1} s^{-1} (*5*). Since monomeric actin binds the actin filament barbed end with a diffusion-limited rate constant of 10 μM^{-1} s^{-1} (*33*), it seems reasonable to assume that profilin also binds to the actin filament barbed end with a

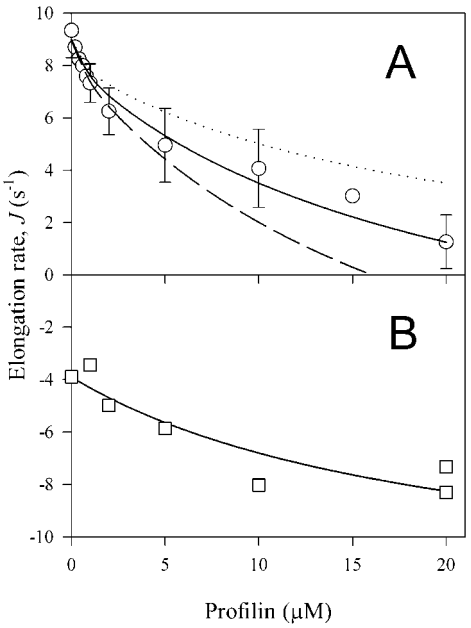

FIGURE 4: Profilin interaction with the actin filament barbed end increases the actin depolymerization rate constant. (A) Elongation of 1 μM MgATP−actin initiated by the addition of spectrin seeds, 100 mM KCl, and 2 mM $MgCl_2$ in the presence of varying profilin concentrations and followed by light scattering. Elongation rate error bars represent the standard deviation of 2−5 measurements. The lines show the calculated values using eq 8 and $k_{AF} = 10\ \mu M^{-1}\ s^{-1}$, $k_{PAF} = 9\ \mu M^{-1}\ s^{-1}$, $k_{-AF} = 1\ s^{-1}$, and different values for k_{-PAF}: dotted line, $k_{-PAF} = 1\ s^{-1}$; solid line, $k_{-PAF} = 5.5\ s^{-1}$; dashed line, $k_{-PAF} = 10\ s^{-1}$. (B) F-actin polymerized from 1% pyrene-labeled MgATP−actin with 100 mM KCl, 2 mM $MgCl_2$, and spectrin seeds diluted 20-fold into F-buffer containing 1 μM DNase I and varying profilin concentrations. The line is a fit to the data using eq 9, yielding $k_{-AF} = 3.9\ (\pm 0.5)\ s^{-1}$ and $k_{-PAF} = 12.6\ (\pm 1.2)\ s^{-1}$. In panels A and B, profilin binding to actin filament barbed ends was calculated using eq 5 and $K_{PF} = 20\ \mu M$.

similar diffusion-limited rate constant. If k_{PF} is estimated to be equal to that for binding to monomeric actin (*5*), then the dissociation rate constant for profilin from the actin filament barbed end is $k_{-PF} = K_{PF} \times k_{PF} = 20\ \mu M \times 15\ \mu M^{-1}\ s^{-1} = 300\ s^{-1}$.

Profilin Binding to the Actin Filament Barbed End Increases the Terminal Actin Subunit Dissociation Rate Constant from the Filament End. The actin elongation rate, *J*, is a function of the both the association and dissociation reactions (eq 8), and provides information about the dissociation rate constant from the actin filament. Determinations of k_{-PAF} for ATP−actin must be inferred from elongation rate measurements (Figure 4A) or shifts in c_{ss} (Figure 2) because ATP hydrolysis and P_i release after actin polymerization produce actin filaments that contain mostly ADP−actin subunits at steady-state. Figure 4A shows barbed end elongation rates for 1 μM β,γ-MgATP−actin in the presence of varying profilin concentrations. The solid line in Figure 4A represents the elongation rates calculated using eq 8, with $k_{AF} = 10\ \mu M^{-1}\ s^{-1}$ (*29*), $k_{PAF} = 9\ \mu M^{-1}\ s^{-1}$ (from Figure 3), $k_{-AF} = 1\ s^{-1}$ (from Figures 1B and 2), leaving one rate constant which was determined by a fit to the data, $k_{-PAF} = 5.5\ s^{-1}$. Also shown are similar calculations using different values for k_{-PAF}: dotted line, $k_{-PAF} = 1\ s^{-1}$; dashed line, $k_{-PAF} = 10\ s^{-1}$. The data indicate that in the absence of profilin, actin monomers dissociate from the filament with a rate constant $k_{-AF} = 1\ s^{-1}$, and in the presence of increasing profilin concentrations, profilin binds to the actin filament barbed ends and the resulting dissociation of PA from the filament end has a rate constant $k_{-PAF} = 5.5\ s^{-1}$.

Figure 4B shows data for direct measurements of depolymerizing actin filaments that yield the rate of ADP−actin dissociation. Light scattering measurements of depolymerizing actin filaments proved to be very noisy (especially at early time points) and difficult to accurately quantify, so actin labeled with pyrene iodoacetamide at low stoichiometry (1%) was used. Even though profilin binds pyrene-actin more weakly than native actin, for short-duration kinetic experiments, pyrene-actin fluorescence is a reliable indicator of polymerization (*18*). F-actin polymerized from spectrin seeds was diluted 20-fold into buffer containing 100 mM KCl, 2 mM $MgCl_2$, 1 μM DNase I, and varying concentrations of profilin, and the rates of disassembly were measured and expressed as negative elongation rates. The presence of DNase I prevents reassociation of monomeric actin with the filaments ends (*30*) and helps to provide a true measurement of the actin dissociation rate from the filament. The solid line in Figure 4B is a fit to the data using eq 9 with $K_{PF} = 20\ \mu M$, yielding $k_{-AF} = 3.9\ (\pm 0.5)\ s^{-1}$ and $k_{-PAF} = 12.6\ (\pm 1.2)\ s^{-1}$, where k_{-AF} and k_{-PAF} represent the rate constants for MgADP−actin and profilin−MgADP−actin dissociation from the actin filament barbed end. Profilin binds to the actin filament barbed end, which results in dissociation of PA from the filament with a rate constant greater than that for actin alone.

It should be noted that although profilin binds to the actin filament barbed end and blocks elongation (Figure 3B), profilin does not cap actin filaments in the traditional sense, because it does not prevent depolymerization of actin monomers from the actin filament barbed end; indeed, the data in Figure 4 indicate that profilin binding to the actin filament barbed end *increases* the actin depolymerization rate. The experiments shown in Figure 4 also reveal that profilin binds to actin filament barbed ends containing either ATP−actin or ADP−actin.

ATP Hydrolysis Is Not Necessary for Elongation of Profilin−Actin. It has been suggested that profilin−actin polymerization requires the coupled hydrolysis of actin-bound ATP (*18*). We tested this hypothesis by polymerizing MgADP−actin in the presence of profilin. Figure 5 shows the F-actin concentrations and elongation rates for 5 μM MgADP−actin in the presence of various profilin concentrations. Because the profilin concentration cannot be considered constant during the time courses of the MgADP−actin elongation reactions, the simpler equations derived for the MgATP−actin experiments (eqs 6−8) cannot be used to describe this series of MgADP−actin polymerization experiments. For comparison, the solid gray lines in Figure 5 were calculated from simulated elongation time courses using eqs 10−15 and the rate constants discussed below (see Table 1).

Figure 5A shows equilibrium F-actin concentrations for 5 μM MgADP−actin in the presence of varying profilin concentrations, measured by TRITC-phalloidin binding. The dashed line represents the calculated concentration of steady-state F-actin assuming that the profilin−MgADP−actin complex could not polymerize (i.e., [F-actin] = $[A_{tot}] - c_c$ − [PA]) using eq 4 and $K_{PA} = 0.4\ \mu M$ (*5*) to calculate [PA], and $c_c = 1.7\ \mu M$ (the concentration

Table 1: Summary of Kinetic Constants for Scheme 1 Determined for Nonmuscle β,γ-Actin

	k_{AF} (μM^{-1} s^{-1})	k_{-AF} (s^{-1})	k_{PAF} (μM^{-1} s^{-1})	k_{-PAF} (s^{-1})	k_{PA} (μM^{-1} s^{-1})	k_{-PA} (s^{-1})	k_{PF} (μM^{-1} s^{-1})	k_{-PF} (s^{-1})
MgATP−actin	10	1	9	5.5	15[a]	1.5[a]	15[b]	300[c]
MgADP−actin	2.5	4.25	1.26	12.6	15[a]	6[a]	15[b]	300[c]

[a] Determined in (*5*). [b] Assumed to be equal to k_{PA}. [c] Calculated from $K_{PF} \times k_{PF}$.

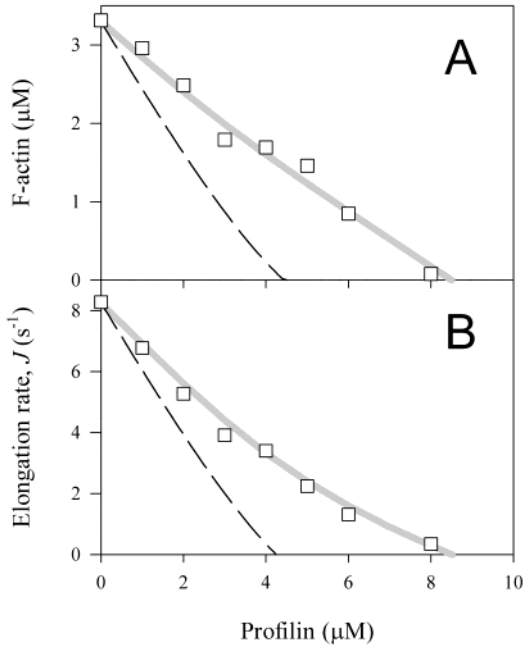

FIGURE 5: Barbed end elongation from MgADP−actin in the presence of profilin. Elongation of 5 μM MgADP−actin was initiated with spectrin seeds, 100 mM KCl, and 2 mM $MgCl_2$ in the presence of varying profilin concentrations. The solid gray lines in panels A and B represent the F-actin concentrations and J values, respectively, calculated from Scheme 1 using eqs 10−15 and constants listed in Table 1. (A) Equilibrium F-actin concentrations for 5 μM MgADP−actin samples measured by TRITC-phalloidin binding. The dashed line is calculated from [F-actin] = $[A_{tot}] - c_c$ − [PA] where c_c = 1.7 μM. (B) Elongation rates for 5 μM MgADP−actin, determined from light scattering time courses. The dashed line represents the elongation rate expected from only MgADP−actin without bound profilin, calculated using eq 3 with k_{AF} = 2.5 μM^{-1} s^{-1} and k_{-AF} = 4.25 s^{-1}. For calculations represented by the dashed lines in panels A and B, profilin binding to actin was calculated using eq 4 with K_{PA} = 0.4 μM.

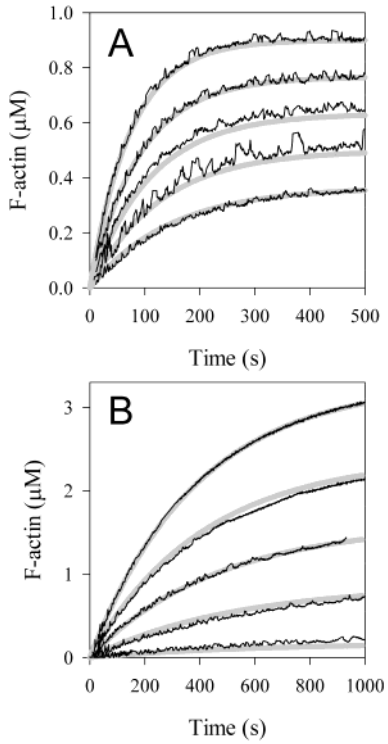

FIGURE 6: Elongation time course data can be described by Scheme 1. Elongation time course data are shown for actin initiated by the addition of spectrin seeds, 100 mM KCl, and 2 mM $MgCl_2$ in the presence of profilin (thin black lines), and simulation based on Scheme 1 (thick gray lines) using equations and constants listed under Materials and Methods and in Table 1 as described in the text. (A) Barbed end elongation of 1 μM MgATP−actin in the presence of, from top to bottom, 0, 5, 10, 15, and 20 μM profilin. (B) Barbed end elongation of 5 μM MgADP−actin in the presence of, from top to bottom, 0, 2, 4, 6, and 8 μM profilin.

of unpolymerized actin at 0 profilin concentration). More F-actin is formed (squares) than expected for a nonpolymerizable profilin−MgADP−actin complex (dashed line), indicating that ATP hydrolysis is not required for actin filament elongation by PA.

Figure 5B shows actin filament barbed end elongation rates for 5 μM MgADP−actin in the presence of varying profilin concentrations. The dashed line represents the calculated contribution of free actin to the elongation rates (eq 3) with the rate constants for MgADP−actin polymerization and depolymerization, k_{AF} = 2.5 μM^{-1} s^{-1} and k_{-AF} = 4.25 s^{-1}, respectively, and where the free actin concentration was calculated using eq 4 and K_{PA} = 0.4 μM (*5*, *34*). If the profilin−MgADP−actin complex were not able to elongate actin filaments, then the elongation would be only via free actin, as described by the dashed line. However, this is not the case; the profilin−MgADP−actin complex does elongate. In other similar experiments not shown, addition of 20 mM P_i to 5 μM MgADP−actin in the presence of profilin increases the equilibrium concentration of F-actin and increases the elongation rate, indicating that P_i slows PA dissociation from the actin filament barbed end, in a manner similar to the known stabilization of F-actin by P_i (*35*).

The Effect of Profilin on the MgATP−Actin and MgADP−Actin Elongation Time Courses Can Be Described by a Global Kinetic Model. Figure 6A,B depicts actin filament barbed end elongation time course data in the presence of varying profilin concentrations using 1 μM MgATP−actin or 5 μM MgADP−actin, respectively (thin black lines). Also depicted in Figure 6 are elongation time course simulations (thick gray lines) calculated using eqs 10−15. The constants used for simulations of MgATP−actin elongation time courses were determined independently from experimental data shown in Figures 1−4 and from previously published data (*5*).

For MgADP−actin, the polymerization constants k_{AF} and k_{-AF} were determined from elongation rates and equilibrium measurements of F-actin, and the profilin binding constants

Table 2: Summary of Equilibrium Constants for Scheme 1 Determined for Different Types of Actin

actin	K_{AF} (μM)	K_{PAF} (μM)	K_{PA} (μM)	K_{PF} (μM)	ϕ[b]	ϕ'[c]	ref
nonmuscle β,γ-ATP−	0.1	0.6	0.1[a]	20	33	1.7	this study
nonmuscle β,γ-ADP−	1.7	10	0.4[a]	20	8.5	0.12	this study
Acanthamoeba ATP−	0.15	0.15	2.5	100	40	5	(*15*)
Acanthamoeba ATP−	0.08	100	0.8	1000	1	0.12	(*17*)
skeletal muscle α-ATP−	0.1	0.1	0.5	7	14	0.5	(*6*)
skeletal muscle α-ATP−	0.12	0.3	0.1				(*31*)
skeletal muscle α-ATP−	0.03	5	1.5	250	1	0.03	(*16*)

[a] Determined in (*5*). [b] ϕ represents the ratio of the equilibrium constants for the two elongation pathways depicted in Scheme 1: $\phi = (K_{AF} \times K_{PF})/(K_{PA} \times K_{PAF})$. [c] $\phi' = \phi \times K_{AN}/K_{PAN}$ where K_{AN} and K_{PAN} are the equilibrium constants for dissociation of nucleotide from actin and from PA, respectively. For nonmuscle β,γ-ATP−actin, $K_{AN}/K_{PAN} = 1/20$ (*5*); for nonmuscle β,γ-ADP−actin, $K_{AN}/K_{PAN} = 1/70$ (*5*); for *Acanthamoeba* ATP−actin, $K_{AN}/K_{PAN} = 1/8$ (*34*); and for skeletal α-ATP−actin, $K_{AN}/K_{PAN} = 1/30$ (*42*).

k_{PA} and k_{-PA} were determined previously in our laboratory (*5*). The dissociation rate constant for PA from the actin filament barbed end, $k_{-PAF} = 12.6\ s^{-1}$, was determined from Figure 4. However, we were not able to independently determine all of the constants used for simulations of MgADP−actin elongation time courses. The values of k_{PF} and k_{-PF} for MgADP−actin were taken to be the same as those determined for actin filaments polymerized from MgATP−actin (from Figure 3). Using these rate constants in the global kinetic model, the one variable, $k_{PAF} = 1.26\ \mu M^{-1}\ s^{-1}$, was derived from fits to the MgADP−actin time course data shown in Figure 6.

The time course simulations describe the data very well and thus support the validity of Scheme 1. Moreover, the global kinetic simulation of the MgATP−actin elongation time course data supports the assumptions made for the simplified analysis of the MgATP−actin data (described under Materials and Methods) that the free profilin concentration can be considered constant during the elongation time course.

DISCUSSION

Profilin Binding to the Actin Filament Barbed End. Our determination of $K_{PF} = 20\ \mu M$ for β,γ-actin represents a 200-fold weaker affinity of profilin for the actin filament barbed end than for monomeric actin. This implies a significant conformational difference between an actin monomer free in solution and an actin subunit bound to an actin filament barbed end. This change in actin affinity for profilin may be similar to the negative cooperativity reported between DNase I and profilin for binding to actin (*36*). Binding of DNase I to the pointed end (subdomains 2 and 4) of the actin monomer weakens profilin binding at another site located at the actin monomer barbed end (subdomains 1 and 3) (*36*). DNase I has been considered an actin analogue because some of the interactions between DNase I and actin are similar to actin−actin interactions within an actin filament (*37*). We interpret our results as indicating negative cooperativity between profilin and the actin filament barbed end for binding monomeric actin. Thus, we agree with the proposal by Tilney et al. (*38*), that an actin conformational change upon association with the actin filament barbed end changes the affinity of actin for profilin.

Dissociation of Profilin−Actin from the Actin Filament Barbed End. Table 2 lists the reported equilibrium dissociation constants for PA binding to the actin filament barbed end, K_{PAF} (*6, 15−17*). Our measurement of the increased actin depolymerization rate in the presence of profilin (Figure 4B) is the first direct evidence that profilin binds to the actin filament barbed end and increases the actin dissociation rate constant. This suggests that profilin binding to an actin subunit induces an actin conformational change that weakens the actin−actin bonds involving the terminal actin subunit in the actin filament. Previous work suggested that profilin binding changes the conformation of monomeric actin, opening the central nucleotide-binding cleft (*5*). Two distinct crystal structures of the profilin−actin complex in "open" and "closed" states also support the idea of a profilin-induced actin conformational change (*4, 39, 40*).

ATP Hydrolysis Is Not Required for Profilin−Actin Elongation. Carlier and co-workers (*6, 18*) postulated that the hydrolysis of ATP by actin initiated upon polymerization of PA decreases the affinity of actin for profilin, releasing profilin from the actin filament barbed end. This assertion is not supported by our data that show elongation of profilin−MgADP−actin (Figures 5 and 6B) by both rate and equilibrium measurements. In agreement with our data, a recent report by Blanchoin and Pollard demonstrates that actin filaments elongate from profilin−ATP−actin faster than the F-actin ATP hydrolysis rate (*41*). Although profilin attenuates actin filament elongation from MgADP−actin more than elongation from MgATP−actin, this would be expected from a competitive binding argument, as shown by Korenbaum et al. (*19*) using profilin mutants with varying actin affinities; elongation from MgADP−actin is an energetically less favorable reaction than elongation from MgATP−actin and is more easily disrupted by profilin binding.

Free Energy Changes for the Elongation Pathways. If the two pathways depicted in Scheme 1 are correct, then the free energy change for the AF pathway, ΔG_{AF}, must equal the free energy change for the PAF pathway, ΔG_{PAF}, and $\Delta\Delta G = \Delta G_{AF} - \Delta G_{PAF} = 0$, where

$$\Delta G_{AF} = -RT \cdot \ln\left(\frac{1}{K_{AF}}\right)$$

$$\Delta G_{PAF} = -RT \cdot \ln\left(\frac{K_{PF}}{K_{PA} \cdot K_{PAF}}\right)$$

Thus, from energetic considerations, the ratio of the constants describing each pathway, ϕ, must equal 1 where: $\phi = (K_{AF} \times K_{PF})/(K_{PA} \times K_{PAF})$. This calculation is listed in Table 2 for several other previous studies and also the present report. Based on the constants in Scheme 1, we find that for β,γ-MgATP−actin, $\phi = 33$, and $\Delta\Delta G = 8.7\ kJ \cdot mol^{-1}$, indicating a more favorable reaction through the PAF

pathway than through the AF pathway. This finding of thermodynamic imbalance is in agreement with that of Pollard and Cooper (*15*) and Pantaloni and Carlier (*6*) but is in disagreement with Pring et al. (*17*) and Kang et al. (*16*). Similar analysis of our data for β,γ-MgADP−actin yields $\phi = 8.5$, which still indicates an imbalance between the two pathways even in the absence of ATP hydrolysis.

Although the constants determined for the reactions in Scheme 1 describe the observed data quite well, the free energy changes for the two pathways are not equal. This leads us to reason that the reaction scheme is not complete. Others have postulated that the energy of ATP hydrolysis by actin (for ATP hydrolysis, $\Delta G = -30$ kJ·mol^{-1}) was responsible for driving the elongation of PA (*6, 18*). An alternative explanation for the apparent energy imbalance could be that the products measured are not the same for both pathways. The greater $-\Delta G_{PAF}$ calculated for actin filament formation from PA suggests that the final free energy state for those actin filaments might be lower that that for actin filaments formed from actin alone. It is possible that the molecular bonds within the polymer are not the same (perhaps transiently) for actin filaments formed from PA. For example, crystal structures have shown that PA can form a ribbon structure that involves actin−actin contacts different from those found in an actin filament (*4*).

Another explanation for the apparent energy imbalance that should be considered is the effect of profilin on nucleotide binding by actin. We have previously shown that profilin reduces the affinity of β,γ-actin for ATP by 20-fold (*5*). If we include the destabilization of ATP binding by actin induced by profilin binding to ATP−actin, then for the reaction P + A ↔ PA, the favorable free energy change produced by the binding of profilin to actin will be offset by the weakening of ATP binding by PA:

$$\Delta G_{PA} = -RT\cdot\ln\left(\frac{1}{K_{PA}}\right) + RT\cdot\ln\left(\frac{K_{AN}}{K_{PAN}}\right)$$

where K_{AN} is the equilibrium dissociation constant for nucleotide binding to actin, K_{PAN} is the equilibrium dissociation constant for nucleotide binding to PA, and for β,γ-ATP−actin $K_{AN}/K_{PAN} = 1/20$. Thus, we can calculate an overall equilibrium constant for dissociation of ATP and profilin from actin, $K_{PA} \times (K_{PAN}/K_{AN}) = 0.1\ \mu M \times 0.13\ \mu M/0.007\ \mu M = 2\ \mu M$, and $\Delta G_{PA} = -33$ kJ·mol^{-1}. Figure 7 illustrates this modification of Scheme 1, and lists the rate and equilibrium constants determined for elongation of β,γ-MgATP−actin in the presence of profilin. Including the constants for nucleotide binding to actin and PA, we can define the ratio of the equilibrium constants for the two elongation pathways as $\phi' = \phi \times K_{AN}/K_{PAN} = 33 \times (1/20) = 1.7$, close to the ideal value of 1. Moreover, free energy calculations yield $\Delta\Delta G = 1$ kJ·mol^{-1}, close to equal energy changes for the two pathways.

The determination of the energy balance involves several constants, each of which adds some error to the final calculation. The values for the actin critical concentration (K_{AF}) and for profilin binding to monomeric actin (K_{PA}) have been measured independently, and our estimates of error for these constants are low and are a small fraction of the values reported. The error estimates are greater for the equilibrium constant for profilin binding to the actin filament barbed end, K_{PF} (Figure 3B), and the rate constant for dissociation of PA from the actin filament barbed end, k_{-PAF} (Figure 4B). In Figures 3B and 4A, we have depicted fits with a range of K_{PF} and k_{-PAF} values to estimate the overall error. We conservatively estimate the overall error for the Scheme 1 energy square to be about a factor of 4. The error for the modified Scheme 1 (Figure 7) will be somewhat larger given the inclusion of other constants. Therefore, the ϕ' value for MgATP−actin of 1.7 is consistent with thermodynamic balance considering our error estimates.

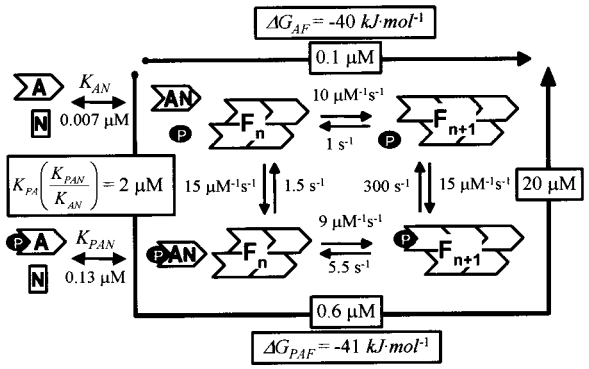

FIGURE 7: Modified scheme for elongation of actin in the presence of profilin. The rate and equilibrium constants determined for elongation of β,γ-MgATP−actin in the presence of profilin are shown. The scheme also depicts the binding of nucleotide, N, to actin and profilin−actin where K_{AN} and K_{PAN} are the respective nucleotide equilibrium dissociation constants. The calculation of the free energy change for the PAF pathway, ΔG_{PAF}, includes the affinities of actin and profilin−actin for nucleotide as described in the text. In this model, the two elongation pathways are energetically equal.

For the case of ADP−actin, profilin binding to actin destabilizes ADP binding by actin by a factor of 70 (*5*); therefore, $\phi' = \phi \times (K_{PAN}/K_{AN}) = 8.5 \times (1/70) = 0.12$. This calculation for MgADP−actin is equivocal; $\phi' = 0.12$ is out of energetic balance to approximately the same magnitude as the value of $\phi = 8.5$ (from Table 2), but indicates a more favorable polymerization by the AF pathway. The failure to unambiguously balance the MgADP−actin energetics may be due to our inability to accurately determine all the pertinent constants; for example, K_{PF} for MgADP−actin was not measured, but assumed to be equal to that for MgATP−actin.

The nucleotide affinities of PA determined for *Acanthamoeba* (*34*) and rabbit skeletal muscle α-actin (*42*) have been used to calculated appropriate ϕ' values and are listed in Table 2. It is interesting to note that for the reports of the thermodynamic imbalance of Scheme 1 (*6, 15*), calculations of ϕ indicate a more favorable reaction through the PAF pathway than through the AF pathway. Moreover, calculations of ϕ' are closer to a thermodynamically balanced state than are calculations of ϕ. While such energetic calculations do not prove that a modified Scheme 1 including nucleotide binding by actin is correct, they offer a rationalization as to why constants from several laboratories were apparently out of thermodynamic balance yet described observed actin elongation time course data. Further work is planned to establish the validity of this hypothesis.

Implications for Profilin Function in Vivo. If actin polymerizes from a large pool of PA in a cell, the free profilin concentration could increase enough to inhibit further actin

filament elongation. This points to the possible importance of PIP_2 binding by profilin [which blocks actin binding by profilin (*43*)] if high concentrations of free profilin are generated by actin polymerization near the plasma membrane. When actin filaments become uncapped, a high free profilin concentration could increase the actin filament depolymerization rate from the barbed end. High profilin concentrations inhibit both the rate and extent of nucleated β,γ-actin polymerization to a much greater degree than α-skeletal muscle actin. Since β-actin is located at the leading edge of moving cells (*20*, *21*), the actin isoform-specific interactions with profilin may be important for regulation of cell motility.

REFERENCES

1. Yang, C., Huang, M., DeBiasio, J., Pring, M., Joyce, M., Miki, H., Takenawa, T., and Zigmond, S. H. (2000) *J. Cell Biol. 150*, 1001−1012.
2. Suetsugu, S., Miki, H., and Takenawa, T. (1998) *EMBO J. 17*, 6516−6526.
3. Wolven, A. K., Belmont, L. D., Mahoney, N. M., Almo, S. C., and Drubin, D. G. (2000) *J. Cell Biol. 150*, 895−904.
4. Schutt, C. E., Myslik, J. C., Rozycki, M. D., Goonesekere, N. C. W., and Lindberg, U. (1993) *Nature 365*, 810−816.
5. Kinosian, H. J., Selden, L. A., Gershman, L. C., and Estes, J. E. (2000) *Biochemistry 39*, 13176−13188.
6. Pantaloni, D., and Carlier, M. F. (1993) *Cell 75*, 1007−1014.
7. Didry, D., Carlier, M. F., and Pantaloni, D. (1998) *J. Biol. Chem. 273*, 25602−25611.
8. Theriot, J. A., Rosenblatt, J., Portnoy, D. A., Goldschmidt-Clermont, P. J., and Mitchison, T. J. (1994) *Cell 76*, 505−517.
9. Geese, M., Schluter, K., Rothkegel, M., Jockusch, B. M., Wehland, J., and Sechi, A. S. (2000) *J. Cell Sci. 113*, 1415−1426.
10. Machner, M. P., Urbanke, C., Barzik, M., Otten, S., Sechi, A. S., Wehland, J., and Heinz, D. W. (2001) *J. Biol. Chem. 276*, 40096−40103.
11. Laurent, V., Loisel, T. P., Harbeck, B., Wehman, A., Grobe, L., Jockusch, B. M., Wehland, J., Gertler, F. B., and Carlier, M. F. (1999) *J. Cell Biol. 144*, 1245−1258.
12. Schluter, K., Jockusch, B. M., and Rothkegel, M. (1997) *Biochim. Biophys. Acta 1359*, 97−109.
13. Mullins, R. D. (2000) *Curr. Opin. Cell Biol. 12*, 91−96.
14. Purich, D. L., and Southwick, F. S. (1999) *Methods Enzymol. 308*, 93−111.
15. Pollard, T. D., and Cooper, J. A. (1984) *Biochemistry 23*, 6631−6641.
16. Kang, F., Purich, D. L., and Southwick, F. S. (1999) *J. Biol. Chem. 274*, 36963−36972.
17. Pring, M., Weber, A., and Bubb, M. R. (1992) *Biochemistry 31*, 1827−1836.
18. Perelroizen, I., Didry, D., Christensen, H., Chua, N. H., and Carlier, M. F. (1996) *J. Biol. Chem. 271*, 12302−12309.
19. Korenbaum, E., Nordberg, P., Bjorkrgren-Sjogren, C., Schutt, C. E., Lindberg, U., and Karlsson, R. (1998) *Biochemistry 37*, 9274−9283.
20. Hoock, T. C., Newcomb, P. M., and Herman, I. M. (1991) *J. Cell Biol. 112*, 653−664.
21. Herman, I. M. (1993) *Curr. Opin. Cell Biol. 5*, 48−55.
22. Rozycki, M., Schutt, C. E., and Lindberg, U. (1991) *Methods Enzymol. 196*, 100−118.
23. Selden, L. A., Kinosian, H. J., Estes, J. E., and Gershman, L. C. (2000) *Biochemistry 39*, 64−74.
24. Kouyama, T., and Mihashi, K. (1981) *Eur. J. Biochem. 114*, 33−36.
25. Gershman, L. C., Selden, L. A., Kinosian, H. J., and Estes, J. E. (1989) *Biochim. Biophys. Acta 995*, 109−115.
26. Lin, D. C., and Lin, S. (1978) *J. Biol. Chem. 253*, 1415−1419.
27. Casella, J. F., Maack, D. J., and Lin, S. (1986) *J. Biol. Chem. 261*, 10915−10921.
28. De La Cruz, E., and Pollard, T. D. (1994) *Biochemistry 33*, 14387−14392.
29. Pollard, T. D. (1986) *J. Cell Biol. 103*, 2747−2754.
30. Mannherz, H. G., Goody, R. S., Konrad, M., and Nowak, E. (1980) *Eur. J. Biochem. 104*, 367−379.
31. Gutsche-Perelroizen, I., Lepault, J., Ott, A., and Carlier, M. F. (1999) *J. Biol. Chem. 274*, 6234−6243.
32. Carlier, M. F., Pantaloni, D., and Korn, E. D. (1984) *J. Biol. Chem. 259*, 9983−9986.
33. Drenckhahn, D., and Pollard, T. D. (1986) *J. Biol. Chem. 261*, 12754−12758.
34. Vinson, V. K., De La Cruz, E. M., Higgs, H. N., and Pollard, T. D. (1998) *Biochemistry 37*, 10871−10880.
35. Carlier, M. F., and Pantaloni, D. (1988) *J. Biol. Chem. 263*, 817−825.
36. Ballweber, E., Giehl, K., Hannappel, E., Huff, T., Jockusch, B. M., and Mannherz, H. G. (1998) *FEBS Lett. 425*, 251−255.
37. Holmes, K. C., Popp, D., Gebhard, W., and Kabsch, W. (1990) *Nature 347*, 44−49.
38. Tilney, L. G., Bonder, E. M., Coluccio, L. M., and Mooseker, M. S. (1983) *J. Cell Biol. 97*, 112−124.
39. Chik, J. K., Lindberg, U., and Schutt, C. E. (1996) *J. Mol. Biol. 263*, 607−623.
40. Page, R., Lindberg, U., and Schutt, C. E. (1998) *J. Mol. Biol. 280*, 463−474.
41. Blanchoin, L., and Pollard, T. D. (2002) *Biochemistry 41*, 597−602.
42. Selden, L. A., Kinosian, H. J., Estes, J. E., and Gershman, L. C. (1999) *Biochemistry 38*, 2769−2778.
43. Lassing, I., and Lindberg, U. (1985) *Nature 314*, 472−474.

BI016083T